

Optical Pumping System Design for Large Production of Hyperpolarized ^{129}Xe

I. C. Ruset,* S. Ketel, and F. W. Hersman

Department of Physics, University of New Hampshire, Durham, New Hampshire 03824, USA

(Received 24 August 2005; published 9 February 2006)

We present a design for a spin-exchange optical pumping system to produce large quantities of highly polarized ^{129}Xe . Low xenon concentrations in the flowing gas mixture allow the laser to maintain high Rb polarization. The large spin-exchange rate between Rb and ^{129}Xe through the long-lived van der Waals molecules at low pressure, combined with a high flow rate, results in large production rates of hyperpolarized xenon. We report a maximum polarization of 64% achieved for a 0.3 l/h Xe flow rate, and maximum magnetization output of 6 l/h at 22% polarization. Our findings regarding the polarization dependence on temperature, nitrogen partial pressure, and gas mixture flow velocity are also reported.

DOI: [10.1103/PhysRevLett.96.053002](https://doi.org/10.1103/PhysRevLett.96.053002)

PACS numbers: 32.80.Bx, 32.10.Dk

In addition to their use in fundamental research [1,2] as polarized targets, hyperpolarized noble gases offer great potential as contrast agents for NMR spectroscopy and MRI studies [3–5]. They can be introduced into the body noninvasively and imaged without the side effects of ionizing radiation. Although demonstrated first for ^{129}Xe [6], the applications of hyperpolarized noble gases in MRI were focused mostly on ^3He because of the well-known polarizing methods and high achievable magnetization [7,8]. Helium is biologically inactive when inhaled, limiting the studies to the lung. Xenon is soluble in blood and readily diffuses throughout tissues offering the opportunity of dissolved-state imaging. Xenon displays NMR spectra with chemical shifts that characterize its microscopic or molecular environment [3,9]. It offers longitudinal magnetization that survives seconds to tens of seconds *in vivo*. The temporal, spatial, and spectral distribution is likely to reveal structural and functional attributes. In addition, xenon is naturally abundant, inexpensive, and its anesthetic biological effects are well tolerated [10].

The physics and methodologies for producing hyperpolarized noble gases have been investigated in detail over three decades of research [11,12]. Two isotopes are normally used, ^3He and ^{129}Xe , which present long relaxation times due to their zero quadrupole moment. For xenon, a spin-exchange optical pumping (SEOP) mixture is made up from the natural or isotopically enriched xenon gas to be polarized, Rb vapor, N_2 , and ^4He [13]. N_2 is used to quench the excited Rb atoms to prevent radiation trapping in the optically dense mixture [11]. Large quantities of ^4He are frequently used to pressure-broaden the Rb D_1 absorption line in order to improve the absorption of the relatively broad spectrum of currently available laser-diode sources [14]. The transfer of polarization from optically polarized Rb electron to Xe nucleus occurs through dipole-dipole interactions in two distinct ways: “sudden” binary collisions [15] and “long-lived” Rb-Xe van der Waals molecules resulting from three body collisions [16,17]. The former is pressure independent and dominates at high pressures, the latter is more efficient and increasingly

dominates at lower pressures [18]. The xenon polarization asymptotically approaches a fraction of the Rb polarization, dictated by the Rb-Xe spin-exchange Γ_{SE} , and Xe spin-destruction rate Γ_{SD} : $P_{\text{Xe}}(t) = P_{\text{Rb}} \frac{\Gamma_{\text{SE}}}{\Gamma_{\text{SE}} + \Gamma_{\text{SD}}} \times [1 - e^{-(\Gamma_{\text{SE}} + \Gamma_{\text{SD}})t}]$, where Rb polarization P_{Rb} is given by the spatial average $P_{\text{Rb}} = \frac{\gamma_{\text{op}}}{\gamma_{\text{op}} + \Gamma_{\text{Rb}}}$. To obtain high Rb polarization one needs a much larger pumping rate γ_{op} than the Rb spin-destruction rate Γ_{Rb} , which is dominated by collisions with Xe. This implies that high polarization values are achieved only if low concentrations of Xe are in contact with the Rb for sufficiently long times. With very few exceptions [19], all previous xenon polarizers were designed to operate in the high pressure regime (3–10 bar) in order to increase the laser absorption in Rb [13]. However, high pressure quenches the efficient transfer of spin from Rb to Xe, requiring longer residence times in the polarizer. High throughput can only be achieved by increasing xenon concentration, leading to increased Rb spin-destruction rates. Finally, the optical pumping rate is limited because the heating of the SEOP mixture and Rb reservoir leads to a runaway increase in Rb density [20].

Our conceptual design largely circumvents these trade-offs. Low pressure operation allows the high spin-exchange rates due to van der Waals molecules to dominate. Low xenon concentration allows high rubidium polarization with lower specific laser absorption. High laser utilization is achieved by using a long cell, high Rb density, and counterflowing the SEOP gas in a direction opposite to that of laser propagation. This arrangement achieves high xenon polarization, even at high flow velocity. The resulting short residence time in the polarizer, however, requires an extended separate region for saturating the Rb vapor density. This separation prevents laser heating from altering the rubidium partial pressure.

The experimental setup is over 2 m in height and vertically oriented (Fig. 1). Its main component, the polarizing cell, is a piece of glass with a total length of ~ 1.8 m and can be described in terms of three operational regions: (a) Rb saturation region, (b) laser absorption and SEOP

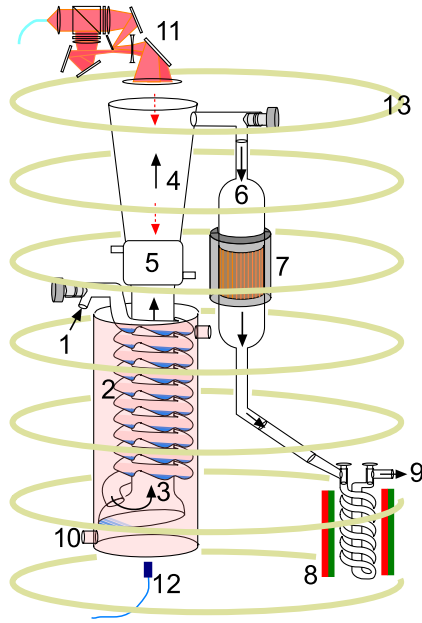


FIG. 1 (color online). Polarizer schematic: (1) gas mixture input coming from the mass flow controllers panel; (2) Rb saturator—spiral shaped containing Rb puddles; (3) SEOP region; (4) Rb condensation region; (5) cooling jacket; (6) down-tube; (7) NMR coils; (8) freezeout spiral inside the 0.3 T permanent magnet box; (9) gas output to pressure controller and exhaust vacuum pump; (10) heating oven; (11) laser and optics; (12) laser monitor spectrometer; (13) B_0 seven-coil tower. The solid arrows show the gas flow in the system, while the dotted arrows show the laser propagation in the column.

region, and (c) Rb condensing region. The lower part of the column which includes the Rb saturator and the SEOP region, ~ 1 m long, is immersed in a pool of hot silicone oil to provide good heat transfer for the SEOP region. The oil is recirculated and maintained at constant temperature. The Rb saturator spiral is made from a ~ 6 m long, 2.5 cm diameter glass tube, with indentations positioned along the tube to hold the Rb puddles. The spiral is initially loaded with 25 g of Rb metal, mostly distributed on its lower half. The long path offered by the spiral allows the gas mixture to reach the oven temperature and achieve a known saturation with Rb vapor independent of flow velocity. The optically thick gas mixture moves from the spiral into the vertical tube and starts flowing upwards against the laser beam coming through the top of the column. The polarization buildup begins at the bottom of the column with the SEOP mixture being illuminated with partially attenuated laser light and progresses as the gas moves towards the more highly illuminated region of the cell. For an ideal case where the Rb density follows strictly the temperature distribution inside the column as shown in Fig. 2, the major laser absorption takes place at the top of the hot region, where the central laser spectrum is absorbed within a few centimeters. As the laser light advances towards the bottom of the column, more and more of its spectrum is absorbed

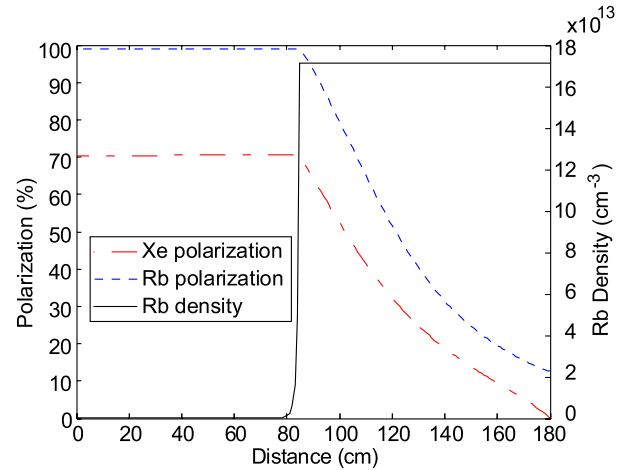


FIG. 2 (color online). Simulated polarization buildup for Xe and Rb inside the polarizer for 10 sccm Xe, 350 sccm N_2 , 1000 sccm He flow rates, and 500 torr total pressure. The gas mixture flows from right to left, with the laser shining from left to right. The temperature is considered uniform at 160 °C inside the oven (85–180 cm on the graph) and drops exponentially to room temperature within 10 cm. Rb density is calculated from the empirical relation of Killian [27].

by the unpolarized Rb atoms. The counterflow of the gas mixture with the laser light in a long cell is critical for an efficient laser absorption as the regions of the cell with lower Rb polarization are never revisited by the highly polarized xenon.

The top half of the column is for cooling the gas mixture to room temperature, allowing Rb condensation to occur while still illuminated by the laser. This part has a conical shape to better match the envelope of the laser beam, starting on top with a 7.5 cm window for laser entrance and tapering to the SEOP region diameter of 4 cm. Cooling of the gas mixture is improved by implementing a 10 cm water cooling jacket above the oven. Visual observations confirmed that most of the Rb is trapped on the walls in this region. After the Rb is completely extracted the remaining gas mixture including the hyperpolarized xenon exits the column through the top stopcock valve into the down-tube. The down-tube makes the transition of the gas mixture from the polarizing column to the base of the polarizer where the spiral freezeout is located. We also implemented an NMR system around this tube as seen in Fig. 1.

Gas flow rates are independently controlled for xenon, N_2 and ^4He with individual mass flow controllers. Total pressure is monitored and controlled using a pressure controller placed before the exhaust vacuum pump. A LABVIEW program interfaces the electronics and monitors the gas flows, pressure, and temperatures.

In order to achieve a high optical pumping rate our polarizer requires high power laser light with narrow spectral bandwidth uniformly illuminating the meterlong polarizing cell. Diode laser technology offers a powerful source of light for Rb SEOP applications. Because the laser is

coupled to a transport fiber, the light becomes unpolarized, and the optics used for beam shaping must also include polarizing components. We developed a new configuration for the optical components which deflects one of the polarization components at an intermediate focus point to provide a uniform circular beam that fits closely our long polarizer column. Typical beam power is ~ 90 W and spectral bandwidth is ~ 1.5 nm FWHM. The laser spectrum and Rb absorption are continuously monitored with a high-resolution optical spectrometer. This optical design and its performance will be presented in detail elsewhere.

Xenon polarization is measured using the standard NMR free induction decay technique. The hyperpolarization is calibrated against proton thermal polarization. A commercial Surrey Medical Imaging Systems MRI console is used for the NMR measurements. Separate drive and receive coils allow independent impedance matching with the signal amplifying electronics. Both coils have transverse cosine-theta configurations and they are enclosed inside a cylindrical Faraday cage. The magnetic field for optical pumping and xenon NMR measurements is chosen at 28.6 G, safely below the range shown to decouple molecular spin exchange [21].

Theoretical simulations implemented in one spatial dimension guided our search for optimal flow rates and operating temperature. Initial tests varying total pressure showed only a slight dependence of the polarization in the range 300–700 torr. Therefore, we decided to operate the system at a constant value of 500 torr. We then explored the ^{129}Xe polarization as a function of the xenon flow rate for several sets of the other parameters. Typically, the total flow is held constant and this is achieved by counterbalancing the xenon flow with ^4He flow, while keeping the N_2 partial pressure also constant. The polarization dependence on the total pressure, N_2 partial pressure, oven temperature, and gas flow velocities was studied in order to find optimum running conditions.

The maximum polarization obtained with our system was 64% at a xenon flow rate of 0.3 liters of xenon per hour. Xenon was polarized also at 50% at 1.2 l/h flow rate, and 22% at 6 l/h. Figure 3 shows our highest numbers obtained at optimum running conditions of 160 °C oven temperature, 500 torr total pressure, 1360 sccm [22] total gas mixture flow, and 350 sccm N_2 flow. In all our studies presented in this Letter we used xenon with natural isotopic abundance. The errors presented are only systematic and dominated by the flow controller readings.

Nitrogen has the main purpose of quenching the Rb excited-state fluorescence. From this point of view there should be a value of the N_2 partial pressure at which the Rb and Xe polarization saturates [23] as the radiation trapping becomes negligible. N_2 has also an effect on the spin-exchange and spin-destruction rates, as N_2 acts as a third body in van der Waals molecule formation [21,24]. We studied the polarization dependence of xenon on the N_2

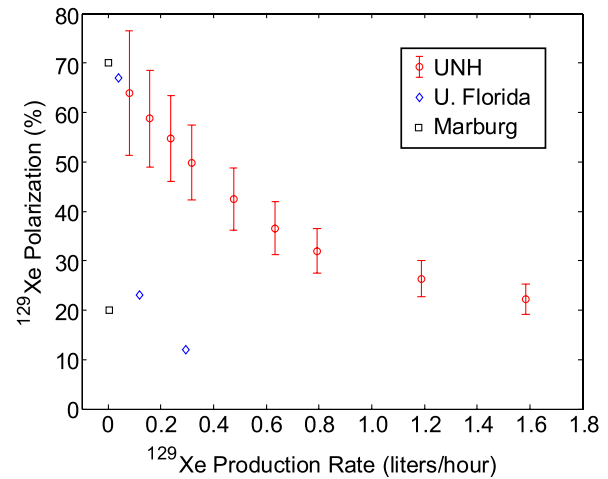


FIG. 3 (color online). ^{129}Xe polarization values produced by the UNH polarizer at optimum experimental parameters. On the graph are also plotted the largest polarization numbers reported in the literature (University of Florida [20] and the Marburg group [19]).

partial pressure. The system was run at 160 °C, with a constant total flow maintained by counterbalancing the flow rates of N_2 and ^4He . We observed a saturation with N_2 above ~ 125 torr partial pressure, which is larger than previously reported values [23] used in polarizing ^3He in sealed cells. For subsequent studies we used N_2 partial pressure of ~ 130 torr.

The temperature of the oil surrounding the Rb saturator spiral dictates the Rb vapor partial pressure of the SEOP mixture. It is important to note that the Rb density is saturated outside the polarizing column, away from the heating effects of the laser [25]. This physical separation prevents the effects of laser heating from vaporizing additional Rb from the liquid reservoir. Unlike Zook *et al.* [20], who report nonlinear Rb density runaway at high laser power, the amount of Rb vapor in our SEOP region remains constant. We mapped the polarization for different temperature settings and concluded that the optimum temperature for our particular system is ~ 160 °C.

Xenon polarization is also dependent on the gas flow velocity. The spin-exchange process requires a minimum amount of time for the Xe to be in contact with Rb vapor in order for Xe polarization to reach saturation. Other local phenomena such as flow turbulence and gas heating due to laser absorption are also dependent on the gas mixture flow velocity. ^4He present in the mixture can be adjusted to control the flow velocity with minimum side effects on the polarizing process. Theoretically there should be an intermediate gas flow velocity where xenon polarization is maximized. We observed an optimum value of total flow of ~ 1350 sccm for 160 °C temperature and 500 torr total pressure, which would correspond to an average flow velocity of ~ 2.8 cm/s in the SEOP region.

TABLE I. Polarization recovery ratios after accumulating and thawing of xenon using the spiral freezeout for different flow rates.

Xenon Flow (sccm)	Accumulated Volume (cm ³)	Recovery Ratio (%)	Absolute Error (%)
10	100	99.8	-17.4
50	500	99.6	-4.7
75	750	92.0	±3.4
100	1000	88.5	±2.8

We also developed a novel approach for accumulating the hyperpolarized xenon. Our new freezeout system consists of a spiral shaped cold trap directing the gas flow downward in the spiral and an adjustable-height liquid nitrogen Dewar. The xenon is uniformly frozen in a thin layer over the walls as the liquid nitrogen level is continuously raised. This configuration minimizes the time spent near the phase transitions, where the relaxation times are very short, of the order of seconds, as well as virtually eliminates the temperature gradients inside the frozen xenon [26]. Using this concept we demonstrated full recovery of polarization after accumulation and thawing for up to 500 cm³ Xe gas. The results are presented in Table I. In the “no phase-transition loss” limit the polarization of the accumulated frozen xenon after the time t_a obeys the relation $P = P_0 \frac{T_1}{t_a} (1 - e^{-t_a/T_1})$, where P_0 is the initial gas polarization, and T_1 is the relaxation time of xenon in frozen state [13]. For $T_1 \sim 2.5$ h [26] and 10 min accumulation time the maximum polarization recovered is 96.7% from initial. While the data in Table I corresponding to 10 and 50 sccm shows values larger than the no phase-transition loss limit, they agree within the experimental uncertainties.

We have described in this Letter a method for producing large quantities of highly polarized ¹²⁹Xe through Rb optical pumping. The advantage of working at low pressure is the large spin-exchange rate between Rb and ¹²⁹Xe, resulting in short residence times for the gas mixture in the SEOP region and large hyperpolarized xenon production. Also, the laser absorption is increased through a novel concept of counterflowing the optical pumping mixture with the laser light over a long optical pumping region. The system is currently providing consistently high output, producing several multiliter batches of hyperpolarized xenon almost daily in a hospital environment.

This work was financially supported by the National Institutes of Health under Grants No. RR14297, No. R15HL67784, No. R01HL073632, and No. EB002553.

*Electronic address: icruset@unh.edu

- [1] W. Xu *et al.*, Phys. Rev. Lett. **85**, 2900 (2000).
 [2] P.L. Anthony *et al.*, Phys. Rev. Lett. **71**, 959 (1993).
 [3] B.M. Goodson, J. Magn. Reson. **155**, 157 (2002).

- [4] A. Cherubini and A. Bifone, Prog. Nucl. Magn. Reson. Spectrosc. **42**, 1 (2003).
 [5] A. Oros and N. Shah, Phys. Med. Biol. **49**, R105 (2004).
 [6] M.S. Albert, G.D. Cates, B. Driehuys, W. Happer, B. Saam, C.S. Springer, and A. Wishnia, Nature (London) **370**, 199 (1994).
 [7] M.E. Wagshul and T.E. Chupp, Phys. Rev. A **49**, 3854 (1994).
 [8] J. Becker *et al.*, Nucl. Instrum. Methods Phys. Res., Sect. A **402**, 327 (1998).
 [9] D. Raftery, H. Long, T. Meersmann, P.J. Grandinetti, L. Reven, and A. Pines, Phys. Rev. Lett. **66**, 584 (1991).
 [10] R. Sanders, D. Ma, and M. Maze, Br. Med. Bull. **71**, 115 (2004).
 [11] W. Happer, Rev. Mod. Phys. **44**, 169 (1972).
 [12] T.G. Walker and W. Happer, Rev. Mod. Phys. **69**, 629 (1997).
 [13] B. Driehuys, G.D. Cates, E. Miron, K. Sauer, D.K. Walter, and W. Happer, Appl. Phys. Lett. **69**, 1668 (1996).
 [14] M.V. Romalis, E. Miron, and G.D. Cates, Phys. Rev. A **56**, 4569 (1997).
 [15] Y.Y. Jau, N.N. Kuzma, and W. Happer, Phys. Rev. A **67**, 022720 (2003).
 [16] N.D. Bhaskar, W. Happer, and T. McClelland, Phys. Rev. Lett. **49**, 25 (1982).
 [17] W. Happer, E. Miron, S. Schaefer, D. Schreiber, W.A. van Wijngaarden, and X. Zeng, Phys. Rev. A **29**, 3092 (1984).
 [18] S. Appelt, A.B. Baranga, C.J. Erickson, M. Romalis, A.R. Young, and W. Happer, Phys. Rev. A **58**, 1412 (1998).
 [19] U. Ruth, T. Hof, J. Schmidh, D. Fick, and H.J. Jansch, Appl. Phys. B **68**, 93 (1999).
 [20] A.L. Zook, B.B. Adhyaru, and C.R. Bowers, J. Magn. Reson. **159**, 175 (2002).
 [21] N.D. Bhaskar, W. Happer, M. Larsson, and X. Zeng, Phys. Rev. Lett. **50**, 105 (1983).
 [22] The measurement sccm is standard cm³ per minute; the physical conditions at which the mass flow controllers were calibrated are considered “standard”: atmospheric pressure and room temperature.
 [23] M.E. Wagshul and T.E. Chupp, Phys. Rev. A **40**, 4447 (1989).
 [24] M. Bouchiat, J. Brossel, and L. Pottier, J. Chem. Phys. **56**, 3703 (1972).
 [25] D.K. Walter, W.M. Griffith, and W. Happer, Phys. Rev. Lett. **86**, 3264 (2001).
 [26] N.N. Kuzma, B. Patton, K. Raman, and W. Happer, Phys. Rev. Lett. **88**, 147602 (2002).
 [27] T. Killian, Phys. Rev. **27**, 578 (1926).